

## A Census Before Rubin of Asteroid Families in the Main Belt

DAVID NESVORNÝ<sup>1</sup>

<sup>1</sup>*Solar System Science & Exploration Division, Southwest Research Institute, 1301 Walnut St., Suite 400, Boulder, CO 80302, USA*

### ABSTRACT

A collisional family is a collection of  $\gtrsim$ km-size asteroid fragments produced by a large scale collision between asteroids. Here we cataloged 335 notable collisional families in the main asteroid belt. When possible, we estimated each family’s formation age, mean visible albedo, taxonomic type, and parent body size. We found that older families ( $t_{\text{age}} > 10$  Myr) produced by impacts on small parent bodies (diameter  $D < 5$  km) are rarely identified because small members of these families have drifted over time by the Yarkovsky effect and blended with the background. The young families ( $t_{\text{age}} < 10$  Myr) typically have small parent bodies ( $D < 10$  km) as large asteroids do not disrupt often enough. The full catalog, including membership files for 335 individual asteroid families, is available for download.<sup>a)</sup>

### 1. INTRODUCTION

The goal of this work is to produce a complete and uniform catalog of asteroid families that can serve as a baseline for future studies with data from the V. Rubin Observatory (Kurlander et al. 2025). We collected known asteroid families from three publications (Nesvorný et al. 2015, 2024, 2026; hereafter P1, P2 and P3). P1 was a synthesis of asteroid families discovered prior to 2015. This publication provided a thorough description of various methods used to identify asteroid families and establish their statistical significance. P2 was a major update of P1 where the proper orbital elements were computed for 1.25 million main belt asteroids. This effort confirmed many families discovered in different studies between 2015 and 2024 (see P2 and P3 for references; also see Novaković et al. 2022). In addition, P2 reported 136 new families. P3 used the proper element catalog from P2 to characterize young asteroid families (formation age  $t_{\text{age}} < 10$  Myr), about 40 known previously and 63 new. All young families were tested in P3 for the past orbital convergence to establish their formation ages. Combining the results of P1, P2 and P3, Table 1 here reports the complete census of asteroid families, 335 main belt families in total.<sup>2</sup>

<sup>a)</sup> <https://www.boulder.swri.edu/~davidn/Proper25>

<sup>2</sup> Additional collisional families were identified among Hildas and Jupiter Trojans. These families require specialized methods to calculate the proper orbital elements. They are not included in the present distribution.

Table 1 has 14 columns: the (1) Family Identification Number, (2-3) number designation and name of an asteroid after which the family is named, (4-5) preferred velocity cutoff (in m/s) and the number of family members identified at this cutoff, (6) family’s taxonomic type, (7) mean visible albedo, (8-9) estimated parent body and largest member diameters (in km), (10) parameter  $C_0$  that defines each family’s V-shape envelope (units of  $10^{-4}$  au; see below), (11-12) estimated family’s formation age and its uncertainty (in Myr), (13) source publications (P1, P2 or P3; see these publications for an extensive list of original references), and (14) a brief comment related to the appearance or location of the family, suspected interlopers, removed/retained large bodies, etc. Below we describe these items in detail.

## 2. ASTEROID FAMILY CATALOG

The full catalog of known asteroid families is reported in Table 1. See <https://www.boulder.swri.edu/~davidn/Proper25> for a machine readable version of Table 1 and the membership files of individual families.

### 2.1. *Family Identification Number*

Table 1 lists the Family Identification Number or FIN in the first column. FIN is our attempt to offer an alternative to the usual standard of family naming convention, where families are named after the lowest numbered, brightest and/or largest member. A problematic facet of the standard convention is the uncertainty to uniquely recognize the lowest numbered, brightest and/or largest member of a family, as it often depends on the adopted cutoff, availability of asteroid size and albedo estimates, etc. (e.g, Masiero et al. 2013). Moreover, the lowest numbered, brightest and largest members in a family may not necessarily be the same object. For these reasons, the existing family-naming convention can be ambiguous in some cases. Our proposal is to define FIN for each known family and use that identification in future publications to assure continuity. The idea is that the FIN designation of a family will stay the same even if there is an urge in the community to rename the family after its (perhaps newly established) largest member. See P1 for the original FIN definition. Here we change the FIN format to accommodate hundreds of new families expected to be identified from the Rubin data.

The main belt is divided into the inner (semimajor axis  $a_P < 2.5$  au), middle ( $2.5 < a_P < 2.82$  au) and outer ( $a_P > 2.82$  au) parts. Given that the proper elements in the P2 catalog have better accuracy for low inclinations, we further divide the main belt into low inclinations ( $\sin i_P < 0.3$ ) and high inclinations ( $\sin i_P > 0.3$ ).<sup>3</sup> The low inclination families are assigned FIN=1XXX (inner belt), FIN=2XXX (middle belt), and FIN=3XXX (outer belt). The high inclination families are assigned

<sup>3</sup> The accuracy of the proper eccentricity,  $e_P$ , in P2 could be improved for  $\sin i_P > 0.3$ , but this is left for a future work.

FIN=4XXX (inner belt), FIN=5XXX (middle belt), and FIN=6XXX (outer belt). Here XXX is a unique family identifier (Table 1 and Figure 1). For example, the Vesta and Flora families have FIN 1001 and 1002. Columns (2) and (3) in Table 1 report the current name of each family which often, but not always, coincides with the largest family member. A secure identification of the largest member in every collisional family should be prioritized in the Rubin era, because that’s fundamental to our understanding of the impact conditions in each case.

## 2.2. Hierarchical Clustering Method

Each family’s membership was defined with the Hierarchical Clustering Method (HCM; Zappalà et al. 1990). The HCM links neighbor orbits in proper element space and requires that family members are linked together with segments shorter than  $d_{cut}$ , where the units of  $d_{cut}$  are m/s (see P1 for a detailed description). Using the methods described in P1, P2 and P3, we tested different  $d_{cut}$  values to establish the preferred value for each family. The preferred HCM cutoff is listed in column (4) of Table 1. Column (5) reports the number of family members identified with this cutoff. Note that the cutoff was fine-tuned for each family to allow for the most reasonable definition in each case. In a handful of cases (e.g., the Flora family, FIN 1002) we also adopted an additional cut in proper element space to separate the family in question from neighbor families. In some cases, where large HCM members of a family were clearly offset from the rest of the family in  $a_P$ ,  $e_P$  and/or  $i_P$ , these large (suspected) interlopers were removed. If so, the exact circumstances of that are noted in column (14) in Table 1.

## 2.3. Taxonomy and Mean Visual Albedo

The visual albedos  $p_V$  of family members were obtained from NEOWISE (Mainzer et al. 2019). We report the mean visual albedo of each family, computed as an average over all family members for which the NEOWISE data were available, in column (7). If the NEOWISE albedo was not available for any of the identified members, we provisionally adopted  $p_V = 0.21$  in the inner main belt,  $p_V = 0.16$  in the middle belt, and  $p_V = 0.1$  in the outer belt, to crudely respect the albedo gradient across the main belt (Mainzer et al. 2019). The taxonomic class, when available, is given by the usual capital letter designation (e.g., C for carbonaceous, S for ordinary chondritic, V for basaltic; DeMeo et al. 2009) in column (6). These designations were taken from P1; they can be improved from more recent taxonomic catalogs but this effort is left for future work. When the taxonomic class of a family was not available from previous publications, we provisionally reported “c” in column (6) for  $p_V \leq 0.08$ , “x” for  $0.08 < p_V \leq 0.15$ , and “s” for  $p_V > 0.15$ . If the taxonomic class and mean albedo were both not available, we reported “x” in column (6). In some cases, noted in column (14), if a small family was found to be located inside a larger background family, the taxonomic type and

albedo of the background family were used to define the values reported in columns (6) and (7) for the small family.

#### 2.4. *Parent Body and Largest Member*

The absolute magnitudes from the Minor Planet Center (MPC), as reported in the family membership files (section 2.7), and the mean albedo from column (7) were converted into a diameter estimate for each identified member. The largest asteroids in every HCM family were inspected, using various criteria based on their proper orbits and position relative to the V-shape envelope in  $(a_P, H)$  (see the next section), to establish whether they likely represent the true largest member in the family (or a possible interloper). When the case was clear, for example when the V envelope was uniquely defined and a large interloper asteroid was located way outside the envelope, we removed it (see notes in column (14) of Table 1). The next largest asteroid centered in the V envelope was then assumed to be the true largest family member. Its diameter  $D_{LM}$  is reported in column (9). Column (9) lists “-1” as a label for ambiguous cases, where there are several, similar-size large asteroids in the HCM family, or if the interpretation is not clear (e.g., a poorly defined V envelope). These cases should be investigated in more detail in the future.

Note that there is a bias in favor of unique interpretation of the families produced by large cratering impacts, where the largest member is often centered in the V envelope and has no competitors. More disruptive collisions, which may produce several large fragments, are generally more difficult to characterize, especially for large families, where some of the large HCM members are expected to be interlopers.

The parent body diameter estimate ( $D_{PB}$ ), reported in column (8), was obtained by adding the volume of all identified fragments together and computing the diameter of an equivalent sphere with the corresponding total volume. The great majority of identified families have  $f = (D_{LM}/D_{PB})^3 \sim 1$ , indicating large cratering (i.e., sub-catastrophic) impacts. The Gefion family in the middle main belt (FIN 2016) corresponds to one of the most disruptive collisions unambiguously identified so far with  $f \simeq 0.013$  (i.e., super-catastrophic impact). In reality, the  $D_{PB}$  value reported in column (8) in Table 1 represents a lower bound on the parent body size, because it does not account for yet-to-be-identified, sub-km family members, which may at least in some cases significantly contribute to the total volume.

#### 2.5. *V-Shape Envelope*

The “V” shape of a great majority of identified asteroid families becomes apparent when the absolute magnitude  $H$  of family members is plotted against the proper semimajor axis  $a_P$ . The V shape results from two processes. First, larger (smaller) fragments tend to be ejected at lower (higher) speeds and thus tend to be initially located, on average, closer to (further away from) the family

center. If the ejection speeds follow  $\delta V \propto 1/D$ , as found for young families (Michel et al. 2015) and laboratory impact experiments (e.g., Fujiwara et al. 1989), the fragments will initially have a V-shape distribution in  $(a_P, H)$ . The envelope of this distribution is given by  $|a_P - a_c| = C_{EV}10^{H/5}$ , where the constant  $C_{EV}$  is related to the magnitude of the ejection velocities (e.g., larger  $C_{EV}$  values are expected for larger parent bodies).

The second, and typically more dominant effect for older families is the Yarkovsky drift (Vokrouhlický et al. 2015). The semimajor axis drift by the Yarkovsky effect is generally given as  $da_P/dt = \text{const.} \times \cos \theta / (a_P D)$ , where  $t$  is time and  $\theta$  is the asteroid obliquity. The maximum drift occurs for  $\theta = 0^\circ$  or  $\theta = 180^\circ$ . Thus, the envelope of the distribution of family members in  $(a_P, H)$  is expected to follow  $|a_P - a_c| = C_{YE}10^{H/5}$ , where  $a_c$  is the family center, often coinciding with the largest family member, and  $C_{YE}$  is a constant related to family's age.<sup>4</sup>

These considerations allow us to define the V-shape envelope as

$$|a_P - a_c| = C_0 \times 10^{H/5}, \quad (1)$$

where  $C_0 \simeq C_{YE} + C_{EV}$ . For young families ( $t_{\text{age}} \lesssim 10$  Myr), for which the effect of ejection speeds dominates,  $C_0$  constrains the ejection velocities and can be used to identify large interlopers as they fall outside the V envelope in  $(a_P, H)$  (P1). For old families ( $t_{\text{age}} > 500$  Myr), for which the Yarkovsky effect dominates,  $C_0$  is typically related to family's formation age (older families will have the V envelopes more open; see Section 2.6). For the intermediate-age families, both effects can be important, and more sophisticated methods need to be employed to separate them (e.g., the Yarkovsky-YORP chronology; Vokrouhlický et al. 2006, Lowry et al. 2020).

Column (10) in Table 1 reports the preferred  $C_0$  value for each family for which the V shape envelope can be reasonably well defined. We experimented with different methods to establish the best-fit  $C_0$  value. In some cases, where the V envelope is well defined, different techniques give essentially the same result (see Figure 2 for an example). Many HCM families, however, have a diffuse structure in  $(a_P, H)$ . In these cases, we found that the correct application of the V-envelope fitting more depends on the choice of  $a_c$ , which is often influenced by the correct identification of the largest members. The procedure is difficult to automate. We therefore inspected each family individually, and made our best choices about the largest family members,  $a_c$  and  $C_0$ . These choices are, for at least some families, subjective – they should be validated (or corrected) when more data become available in the future. These cases are noted in column (14).

<sup>4</sup> See Nesvorný et al. (2003) for some of the early applications of this method. Milani et al. (2014) and Spoto et al. (2015) opted to use the envelope in  $(a_P, 1/D)$ , instead of  $(a_P, H)$ , which is basically the same thing, except it requires that the albedo is known.

## 2.6. Formation Age Estimates

Columns (11) and (12) in Table 1 report the formation age estimates,  $t_{\text{age}}$ , and their uncertainties. We used several sources to collect these values. For the young families, robust age estimates were obtained from the backward convergence of orbital longitudes. This was the subject of P3 – most values reported in column (11) with  $t_{\text{age}} < 10$  Myr were taken from P3. Additionally, we tested all families from P2 for orbital convergence and found eight new convergent families that were not recognized in P3: 2927 Alamosa ( $t_{\text{age}} = 2.2 \pm 1.0$  Myr), 4291 Kodaihasu ( $t_{\text{age}} = 5.0 \pm 1.5$  Myr), 7233 Majella ( $t_{\text{age}} = 1.7 \pm 1.0$  Myr), 8223 Bradshaw ( $t_{\text{age}} = 4.0 \pm 1.0$  Myr), 8272 Iitatemura ( $t_{\text{age}} = 3.0 \pm 1.5$  Myr), 12586 Shukla ( $t_{\text{age}} = 1.5 \pm 1.0$  Myr), 325224 2008GK38 ( $t_{\text{age}} = 4.5 \pm 1.5$  Myr), and 484743 2008YL101 ( $t_{\text{age}} = 0.8 \pm 0.3$  Myr; 484743 does not participate in the orbital convergence and is probably an interloper).

For old families, rough age estimates were obtained from the V envelope. Adopting thermal parameters appropriate for the *S* and *C* type asteroids (Vokrouhlický et al. 2015), we estimated that the maximum Yarkovsky drift of a reference  $D = 1$  km body at  $a = 2.5$  au is  $(da/dt)_S = 1.61_{-0.82}^{+1.67} \times 10^{-4}$  au Myr $^{-1}$  for S, and  $(da/dt)_C = 2.35_{-1.20}^{+2.74} \times 10^{-4}$  au Myr $^{-1}$  for C. For comparison, if the observed Yarkovsky drift for Golevka (S type) and Bennu (C type) are rescaled to the same size and orbital radius, we get  $2.25 \times 10^{-4}$  au Myr $^{-1}$  and  $1.82 \times 10^{-4}$  au Myr $^{-1}$ , respectively. Given these results, we make no distinction between S and C type asteroids, and adopt the drift rate

$$\frac{da}{dt} = 2 \times 10^{-4} \text{ au/Myr} \times \cos \theta \left( \frac{1 \text{ km}}{D} \right) \left( \frac{2.5 \text{ au}}{a} \right)^2. \quad (2)$$

Ignoring  $C_{\text{EV}}$ , the formation age of an old asteroid family can be roughly estimated from

$$t_{\text{age}} \simeq 1500 \text{ Myr} \times \left( \frac{C_0}{10^{-4} \text{ au}} \right) \left( \frac{a}{2.5 \text{ au}} \right)^2, \quad (3)$$

where we adopted the Yarkovsky drifts discussed above, and assumed  $\theta = 0^\circ$  or  $\theta = 180^\circ$ . This relation is similar to Eq. (1) in P1, but here we neglected any dependence on the asteroid bulk density and albedo, and other parameters that determine the strength of the Yarkovsky effect (Vokrouhlický et al. 2015). The systematic impact of these parameters on  $t_{\text{age}}$  is difficult to establish without a detail physical characterization of a large number of asteroid members in each family. In column (12), we therefore often adopt a conservative 50% uncertainty of the age estimate. This should capture the uncertainty in physical parameters but not the one related to the ejection speeds.

The contribution of ejection speeds to the V shape envelope can be substantial. For some families, for which a better age estimate was previously obtained from detailed Yarkovsky-YORP chronology modeling (Vokrouhlický et al. 2006), this better age estimate is reported in columns (11) and (12) of Table 1. This includes the Agnia, Astrid, Baptistina, Clarissa, Eos, Erigone, Gefion, Merxia and

Tina families (see P1 and Lowry et al. 2020). The Yarkovsky-YORP chronology modeling optimizes model parameters (e.g., ejection velocities, YORP strength, family’s age) on the observed family structure in  $(a, H)$ . It is a better approach to the family age estimation than the V-shape envelope method (e.g., Spoto et al. 2015), because it accounts for the contribution of ejection velocities. A comparison of the Yarkovsky-YORP chronology modeling with the V envelope method indicates that the ejection speeds can easily affect the age estimate by  $\sim 50\%$  for younger families (e.g., Agnia, Mexia; Figure 2), and by up to  $\sim 20\%$  for older families (Flora). For the bulk of intermediate-age families, however, the Yarkovsky-YORP chronology modeling is not available (the method was not applied to them). In these cases, we therefore report the V envelope age in column (11) and a 50% uncertainty in column (12). For old families, where the contribution of the ejection velocity field should be less of a factor, column (11) of Table 1 reports the V envelope age from Eq. (3).

### 2.7. Membership Files

The membership files, one file for each family listed in Table 1, report the proper elements  $a_P$  (in au),  $e_P$  and  $\sin i_P$  (columns 1-3), proper secular frequencies  $g$  and  $s$  (in arcsec/yr; columns 4 and 5), absolute magnitude  $H$  from MPC (mag; column 6), number of oppositions (column 7), MPC compact designation and real name (columns 8 and 9) for each family member. See Table 2 for an example. The number of oppositions in column (7) can be used to discard asteroids with poorly determined orbits. The asteroid family distribution available at <https://www.boulder.swri.edu/~davidn/Proper25> also provides the original MPC catalog from which the proper elements were computed in P2 (from February 2024), and the full proper element catalog for 1.25 million main belt asteroids, including uncertainties of  $a_P$ ,  $e_P$  and  $\sin i_P$  (see P2).

## 3. DISCUSSION

Figure 3 shows the distribution of families in  $t_{\text{age}}$ ,  $D_{LM}$  and  $f = (D_{LM}/D_{PB})^3$ , with  $f > 0.5$  and  $f < 0.5$  defining cratering events and catastrophic breakups, respectively (Benz & Asphaug 1999). There are several notable features. First, families above the upper dashed line in Fig. 3 are not expected to be found because large parent bodies do not produce families often enough. In addition, as the ages estimates based on the the V-envelope chronology method (Section 2.6) ignore the initial ejection velocity field, they are artificially shifted to larger values. A good example of this is the Veritas family. The real Veritas family age is  $t_{\text{age}} = 8.3 \pm 0.1$  Myr based on the past orbital convergence (P3). The V-envelope fit, however, gives  $C_0 = 7 \times 10^{-6}$  au, which would then lead to the age estimate of  $\sim 130$  Myr from Eq. (3). This is also probably the reason why there are relatively few families with the estimated formation ages  $\sim 5$ -50 Myr in Fig. 3 – these families have (incorrectly) been assigned older ages from the V-envelope method.

Second, families below the bottom dashed line in Fig. 3 are not identified. This is a consequence of detection bias, because families produced by small parent bodies have small members that rapidly drift in  $a_P$  by the Yarkovsky effect. The drift leads to a significant displacement of family members in  $a_P$  if the small family formed long time ago. Weak resonance crossings further disperse the family members in  $e_P$  and  $i_P$ . As a result, if enough time elapses, the small family members blend with the background and cannot be recognized as an orbital group in proper element space.<sup>5</sup>

Third, the majority of currently known families were produced by cratering impacts with  $f > 0.5$  (blue dots in shown in Fig. 3). This may be expected because the cratering impacts require smaller projectiles and thus happen more often. The families corresponding to catastrophic breakups are often found around smaller parent bodies (red dots in Fig. 3;  $D_{PB} \sim 10$  km), as expected because there are many more smaller asteroids in the main belt, implying a greater opportunity for catastrophic breakups. Interestingly, not many catastrophic breakups were identified around families with  $t_{\text{age}} \lesssim 1$  Myr (see P3 for a discussion). The Gefion and Dora families with  $f = 0.013$  and  $f = 0.035$ , respectively, correspond to two most catastrophic breakup events of large main belt asteroids. The Gefion family was hypothesized to be an important source of (fossil) L chondrite meteorites (but see Marsset et al. 2025). The Dora family can be a notable source of large carbonaceous impactors on the Earth.

## ACKNOWLEDGEMENTS

This work was funded by the NASA SSW program.

## REFERENCES

- Benz, W. & Asphaug, E. 1999, *Icarus*, 142, 1, 5.  
doi:10.1006/icar.1999.6204
- DeMeo, F. E., Binzel, R. P., Slivan, S. M., et al. 2009, *Icarus*, 202, 1, 160.  
doi:10.1016/j.icarus.2009.02.005
- Fujiwara, A., Cerroni, P., Davis, D. R., et al. 1989, *Asteroids II*, 240.
- Kurlander, J. A., Bernardinelli, P. H., Schwamb, M. E., et al. 2025, Predictions of the LSST Solar System Yield: Near-Earth Objects, Main Belt Asteroids, Jupiter Trojans, and Trans-Neptunian Objects, arXiv:2506.02487.
- Lowry, V. C., Vokrouhlický, D., Nesvorný, D., et al. 2020, *AJ*, 160, 3, 127.  
doi:10.3847/1538-3881/aba4af
- Mainzer, A. K., Bauer, J. M., Cutri, R. M., et al. 2019, NASA Planetary Data System, NEOWISE Diameters and Albedos V2.0, 251.  
doi:10.26033/18S3-2Z54
- Marsset, M., Vernazza, P., Brož, M., et al. 2024, *Nature*, 634, 8034, 561.  
doi:10.1038/s41586-024-08007-6
- Masiero, J. R., Mainzer, A. K., Bauer, J. M., et al. 2013, *ApJ*, Asteroid Family Identification Using the Hierarchical Clustering Method and WISE/NEOWISE Physical Properties, 770, 1.  
doi:10.1088/0004-637X/770/1/1

<sup>5</sup> Many families are found to have  $t_{\text{age}} \lesssim 1$  Myr in Fig. 3. These young families are tightly clustered in  $a_P$ ,  $e_P$  and  $i_P$ , sometimes in orbital longitudes as well, and are thus easily recognized. Moreover, the age of young families can be established with the orbital convergence method, effectively proving that the families are real.

- Michel, P., Richardson, D. C., Durda, D. D., et al. 2015, *Asteroids IV*, 341.  
doi:10.2458/azu\_uapress\_9780816532131-ch018
- Milani, A., Cellino, A., Knežević, Z., et al. 2014, *Icarus*, 239, 46. doi:10.1016/j.icarus.2014.05.039
- Nesvorný, D., Bottke, W. F., Levison, H. F., et al. 2003, *ApJ*, 591, 1, 486. doi:10.1086/374807
- Nesvorný, D., Brož, M., & Carruba, V. 2015 (P1), *Asteroids IV, Identification and Dynamical Properties of Asteroid Families*, 297.  
doi:10.2458/azu\_uapress\_9780816532131-ch016
- Nesvorný, D., Roig, F., Vokrouhlický, D., et al. 2024a (P2), *ApJS, Catalog of Proper Orbits for 1.25 Million Main-belt Asteroids and Discovery of 136 New Collisional Families*, 274, 2, 25.  
doi:10.3847/1538-4365/ad675c
- Nesvorný, D., Vokrouhlický, D., Brož, M., et al. 2026 (P3), *Icarus*, 443, 116768.  
doi:10.1016/j.icarus.2025.116768
- Novaković, B., Hsieh, H. H., Cellino, A., et al. 2014, *Icarus*, 231, 300.  
doi:10.1016/j.icarus.2013.12.019
- Novaković, B., Vokrouhlický, D., Spoto, F., et al. 2022, *Celestial Mechanics and Dynamical Astronomy*, 134, 4, 34.  
doi:10.1007/s10569-022-10091-7
- Spoto, F., Milani, A., & Knežević, Z. 2015, *Icarus*, 257, 275. doi:10.1016/j.icarus.2015.04.041
- Vokrouhlický, D., Brož, M., Bottke, W. F., et al. 2006, *Icarus*, 182, 1, 118.  
doi:10.1016/j.icarus.2005.12.010
- Vokrouhlický, D., Bottke, W. F., Chesley, S. R., et al. 2015, *Asteroids IV, The Yarkovsky and YORP Effects*, 509.  
doi:10.2458/azu\_uapress\_9780816532131-ch027
- Vokrouhlický, D., Nesvorný, D., Brož, M., et al. 2024, *A&A*, 681, A23.  
doi:10.1051/0004-6361/202347670
- Vokrouhlický, D., Nesvorný, D., Bottke, W. F., et al. 2026, submitted to *AJ*
- Zappala, V., Cellino, A., Farinella, P., et al. 1990, *AJ*, 100, 2030. doi:10.1086/115658

**Table 1.** 335 families distributed in the Proper25 catalog. See the main text for a description of columns. The machine-readable version of this file is available from <https://www.boulder.swri.edu/~davidn/Proper25>.

(1)	(2)	(3)	(4)	(5)	(6)	(7)	(8)	(9)	(10)	(11)	(12)	(13)	(14)	
							<i>Inner Main Belt, <math>a &lt; 2.5 AU</math>, <math>i &lt; 17.5^\circ</math></i>							
1001	4	Vesta	35	27121	V	0.35	527.0	525.0	1.000	1300.000	800.000	P1	source of HED meteorites	
1002	8	Flora	40	23002	S	0.22	215.0	140.0	1.300	1300.000	500.000	P1	source of LL NEOs, includes Baptistina	
1003	298	Baptistina	37	15922	X	0.21	91.0	16.0	0.170	230.000	90.000	P1	many large interlopers from Flora	
1004	20	Massalia	30	19967	S	0.21	146.0	144.0	0.180	150.000	50.000	P1	source of L chondrites?, $\sin i < 0.03176$	
1005	44	Nysa-Polana	35	38648	SFC	-1.00	-1.0	-1.0	-1.000	-1.000	-1.000	P1	includes Eulalia, $\sin i > 0.03176$ , Bottke et al. (2026)	
1006	163	Erigone	30	3601	CX	0.06	84.0	82.0	0.150	270.000	150.000	P1	cut by a secular resonance	
1007	302	Clarissa	40	812	CB	0.05	43.0	41.0	0.045	60.000	20.000	P1	Lowry et al. (2020)	
1008	752	Sulamitis	40	825	C	0.07	62.0	61.0	0.200	290.000	150.000	P1	-	
1009	1892	Lucienne	80	1525	S	0.20	15.0	12.0	0.100	150.000	80.000	P1	-	
1010	27	Euterpe	50	553	S	0.26	118.0	118.0	0.300	400.000	200.000	P1	onesided	
1011	1270	Datura	10	77	S	0.21	8.2	8.1	-1.000	0.500	0.200	P3	Vokrouhlický et al. (2024)	
1012	21509	Lucascavin	10	3	S	0.21	2.9	2.8	-1.000	0.500	0.300	P3	rotational fission?	
1013	84	Klio	56	84	C	0.07	79.0	79.0	0.300	400.000	200.000	P1	cutoff finetuned, onesided, poorly defined V	
1014	623	Chimaera	100	563	CX	0.08	36.0	34.0	0.280	400.000	200.000	P1	4 Hebe removed	
1015	313	Chaldaea	50	661	C	0.07	96.0	96.0	0.030	40.000	20.000	P1	V shifted relative to 313	
1016	329	Svea	150	436	CX	0.06	69.0	69.0	0.300	440.000	220.000	P1	onesided	
1017	108138	2001GB11	20	47	c	0.05	17.0	16.0	-1.000	3.500	0.500	P3	P/2012 F5	
1018	6	Hebe	80	112	S	0.23	195.0	195.0	0.050	150.000	100.000	P2	V poorly defined	
1019	40	Harmonia	70	160	s	0.26	119.0	119.0	0.040	50.000	25.000	P2	-	
1020	67	Asia	40	569	s	0.26	63.0	63.0	0.170	240.000	120.000	P2	-	
1021	114	Thyra	30	56	s	0.21	55.0	55.0	0.020	30.000	15.000	P2	V poorly defined	
1022	126	Velleda	70	308	s	0.21	41.0	40.0	0.300	430.000	220.000	P2	onesided, V poorly defined	
1023	135	Hertha	20	1473	s	0.22	77.0	77.0	0.100	140.000	120.000	P2	onesided, notable left ear	
1024	345	Tercidina	80	429	s	0.16	157.0	99.0	0.250	320.000	160.000	P2	-	
1025	1156	Kira	70	33	s	0.25	8.9	8.9	0.020	30.000	15.000	P2	V poorly defined, not convergent	
1026	1217	Maximiliana	20	28	s	0.21	7.6	7.5	-1.000	1.100	0.400	P3	-	
1027	1394	Algoa	50	27	x	0.21	13.0	13.0	0.050	70.000	35.000	P2	-	
1028	1598	Paloque	40	117	s	0.20	13.0	10.0	0.100	130.000	65.000	P2	-	
1029	1663	VandenBos	30	285	s	0.29	17.0	12.0	0.020	25.000	15.000	P2	many large interlopers	
1030	2110	Moore-Sitterly	10	17	s	0.19	5.5	5.4	0.002	1.350	0.150	P3	-	

**Table 1** continued on next page

**Table 1** (continued)

(1)	(2)	(3)	(4)	(5)	(6)	(7)	(8)	(9)	(10)	(11)	(12)	(13)	(14)
1031	2328	Robeson	20	223	c	0.06	14.0	12.0	0.012	16.000	6.500	P2	large 20432, not convergent
1032	2728	Yatskiv	30	48	s	0.21	8.3	8.2	0.018	26.000	13.000	P2	not convergent
1033	2653	Principia	50	131	c	0.04	24.0	24.0	0.040	60.000	30.000	P2	two large V envelope interlopers
1034	2823	vanderLaan	60	136	s	0.22	9.2	5.4	0.100	140.000	70.000	P2	2823 may be interloper
1035	2961	Katsurahama	25	142	s	0.16	10.0	7.6	0.100	120.000	60.000	P2	poorly defined V
1036	3452	Hawke	100	116	s	0.40	6.3	3.5	0.300	370.000	135.000	P2	-
1037	6142	Tantawi	30	114	c	0.04	13.0	11.0	-1.000	3.000	1.000	P3	-
1038	8272	Iitatemura	40	41	s	0.20	7.3	7.2	0.015	3.000	1.500	P2	convergent
1039	18429	1994AO1	10	37	c	0.08	11.0	11.0	-1.000	2.000	0.500	P3	-
1040	61203	Chleborad	30	63	x	0.21	5.8	2.6	0.030	44.000	22.000	P2	poorly defined V
1041	118564	2000FO47	20	83	x	0.21	5.2	1.3	0.010	13.000	7.500	P2	not convergent, shifted V
1042	484743	2008YL101	30	16	x	0.21	1.1	0.8	0.002	0.800	0.300	P2	poorly defined V, convergent
1043	0	2012PM61	15	35	x	0.21	0.7	0.7	-1.000	-1.000	-1.000	P2	no V shape, bodies similar in size
1044	525	Adelaide	10	86	x	0.13	11.0	11.0	0.002	0.536	0.012	P3	-
1045	5026	Martes	10	6	x	0.21	4.5	4.5	-1.000	0.018	0.001	P3	-
1046	6825	Irvine	40	10	s	0.29	4.7	4.7	-1.000	1.800	0.500	P3	-
1047	10321	Rampo	10	47	s	0.30	3.9	3.9	-1.000	0.750	0.150	P3	-
1048	10484	Hecht	10	5	v	0.23	5.1	4.6	-1.000	0.250	0.050	P3	in the Vesta family, two interlopers included
1049	11842	Kapbos	10	7	x	0.21	4.1	4.1	-1.000	0.750	0.750	P3	Kap'bos
1050	39991	Iochroma	10	7	x	0.21	3.5	3.4	-1.000	0.350	0.350	P3	double convergence
1051	157123	2004NW5	20	17	c	0.04	4.3	3.9	-1.000	0.100	0.100	P3	some interlopers
1052	1821	Aconcagua	10	5	x	0.21	6.3	6.3	-1.000	0.800	0.200	P3	-
1053	5722	Johnscherrer	10	4	x	0.21	4.0	4.0	-1.000	0.900	0.300	P3	in Flora
1054	7629	Foros	10	3	x	0.21	3.5	3.5	-1.000	0.300	0.100	P3	in Nysa-Polana
1055	8306	Shoko	10	4	x	0.21	2.7	2.7	-1.000	0.400	0.100	P3	in Flora, 8306 is a binary
1056	14155	Cibronen	10	3	s	0.28	3.7	3.7	-1.000	0.500	0.200	P3	in Flora
1057	14161	1998SO145	10	3	x	0.21	2.8	2.8	-1.000	0.700	0.500	P3	-
1058	14798	1978UW4	10	4	x	0.21	4.0	4.0	-1.000	0.350	0.050	P3	in Vesta
1059	15180	9094P-L	10	3	x	0.21	2.6	2.6	-1.000	0.700	0.200	P3	-
1060	23637	1997AM6	10	3	x	0.21	2.2	2.2	-1.000	0.100	0.100	P3	in Vesta
1061	28805	Fohring	10	12	s	0.30	3.5	3.5	-1.000	0.700	0.300	P3	-
1062	30301	Kuditipudi	10	3	x	0.21	2.7	2.7	-1.000	0.500	0.100	P3	in Baptistina
1063	38184	1999KF	10	4	x	0.21	1.9	1.9	-1.000	0.700	0.200	P3	in Euterpe
1064	44938	1999VV50	10	3	x	0.21	2.5	2.5	-1.000	0.250	0.250	P3	-
1065	48939	1998QO8	10	5	x	0.21	2.5	2.5	-1.000	0.300	0.200	P3	in Vesta

**Table 1** continued on next page

Table 1 (continued)

(1)	(2)	(3)	(4)	(5)	(6)	(7)	(8)	(9)	(10)	(11)	(12)	(13)	(14)
1066	50423	2000DE13	10	4	x	0.21	1.8	1.8	-1.000	0.300	0.100	P3	-
1067	70512	1999TM103	10	3	x	0.21	2.7	2.6	-1.000	0.700	0.300	P3	in Vesta
1068	80245	1999WM4	10	3	x	0.21	2.0	2.0	-1.000	0.200	0.100	P3	-
1069	100440	1996PJ6	10	3	x	0.21	1.5	1.5	-1.000	0.150	0.100	P3	in Nysa-Polana
1070	107286	2001BU76	10	3	x	0.21	1.4	1.3	-1.000	0.420	0.050	P3	in Massalia
1071	111298	2001XZ55	10	3	x	0.21	1.6	1.5	-1.000	0.100	0.100	P3	in Nysa-Polana
1072	133302	2003SM45	10	3	x	0.21	1.5	1.5	-1.000	0.100	0.100	P3	in Massalia
1073	141906	2002PJ73	10	3	x	0.21	1.5	1.4	-1.000	1.200	0.500	P3	in Flora
1074	156163	2001TF112	10	3	x	0.21	1.7	1.7	-1.000	1.200	0.300	P3	-
1075	213065	1999RT127	10	3	x	0.21	1.1	1.1	-1.000	1.000	0.500	P3	-
1076	237295	2008YN7	10	6	c	0.05	4.1	3.1	-1.000	0.500	0.500	P3	in Clarissa, 3 interlopers?
1077	237517	2000SP31	10	3	x	0.21	1.3	1.2	-1.000	0.700	0.300	P3	-
1078	353790	2012PE32	10	3	x	0.21	1.2	1.1	-1.000	0.800	0.300	P3	in Nysa-Polana
1079	381362	2008EP15	10	7	x	0.21	0.9	0.6	-1.000	1.000	1.000	P3	-
1080	572119	2008CF225	10	4	x	0.21	0.6	0.6	-1.000	0.500	0.500	P3	-
1081	0	2006SO248	10	6	x	0.21	0.6	0.6	-1.000	0.250	0.250	P3	496607 is interloper
1082	0	2021PE78	10	35	x	0.21	0.7	0.7	-1.000	1.100	0.500	P3	-
<i>Middle Main Belt, <math>2.5 &lt; a &lt; 2.82 AU</math>, <math>i &lt; 17.5^\circ</math></i>													
2001	3	Juno	35	16373	S	0.20	254.0	251.0	0.300	510.000	260.000	P1	cratering, steep SFD, H chondrites?
2002	15	Eunomia	33	13099	S	0.25	281.0	259.0	1.500	2500.000	1250.000	P1	cutoff finetuned
2003	-1	-	-1	-1	-	-1.00	-1.0	-1.0	-1.000	-1.000	-1.000	P1	46 Hestia family removed
2004	128	Nemesis	30	2938	C	0.08	198.0	188.0	0.200	360.000	100.000	P1	128 offset, higher cutoff fails, onesided
2005	145	Adeona	33	7382	C	0.07	160.0	151.0	0.500	860.000	430.000	P1	-
2006	170	Maria	30	1683	S	0.25	63.0	35.0	-1.000	-1.000	-1.000	P1	large 170 may be interloper, see FIN 2054
2007	363	Padua	23	1683	X	0.07	-1.0	-1.0	0.400	720.000	360.000	P1	large 110 Lydia
2008	396	Aeolia	15	1788	X	0.10	38.0	37.0	0.030	54.000	27.000	P1	no ears, too young to have ears?
2009	410	Chloris	55	1071	C	0.10	121.0	119.0	0.600	1100.000	550.000	P1	Chloris offset in $i$ , $\sin i < 0.16158$
2010	569	Misa	35	2811	C	0.06	59.0	54.0	0.080	140.000	70.000	P1	-
2011	606	Brangane	30	1545	TK	0.11	38.0	37.0	0.035	56.000	28.000	P1	V shifted by 0.003 au relative to 606
2012	668	Dora	28	4906	C	0.06	75.0	24.0	0.200	400.000	200.000	P1	poorly defined V
2013	808	Merxia	35	4226	S	0.20	44.0	38.0	0.300	250.000	50.000	P1	V envelope interlopers 1327, 6633, 50694
2014	847	Agnia	25	8374	S	0.19	46.0	30.0	0.150	100.000	50.000	P1	cutoff finetuned, V shifted by 0.01 au
2015	1128	Astrid	50	1585	C	0.05	51.0	45.0	0.120	250.000	100.000	P1	resonant fork in $a,e$
2016	1272	Gefion	35	4807	S	0.23	51.0	12.0	0.700	500.000	200.000	P1	93,255,481 offset and removed, fossil L chondrites?
2017	3815	Konig	30	2611	CX	0.05	33.0	20.0	0.030	50.000	25.000	P1	342 offset and removed

Table 1 continued on next page

Table 1 (continued)

(1)	(2)	(3)	(4)	(5)	(6)	(7)	(8)	(9)	(10)	(11)	(12)	(13)	(14)
2018	1644	Rafita	40	2126	S	0.22	26.0	14.0	0.400	600.000	300.000	P1	Rafita far away, HCMed around 1658 Innes
2019	1726	Hoffmeister	20	5590	CF	0.05	61.0	25.0	0.150	280.000	140.000	P1	-
2020	4652	Iannini	20	3110	S	0.23	22.0	21.0	0.020	6.000	2.000	P3	cratering on 1547 Nele
2021	7353	Kazuya	30	377	S	0.21	11.0	9.2	0.010	2.000	2.000	P3	-
2022	173	Ino	35	2411	S	0.22	71.0	71.0	0.400	720.000	360.000	P1	-
2023	14627	Emilkowalski	10	17	S	0.22	7.4	7.1	-1.000	0.300	0.100	P3	-
2024	16598	Brugmansia	10	3	S	0.16	4.0	3.9	-1.000	0.170	0.060	P3	formerly 1992YC2, rotational fission?
2025	2384	Schulhof	10	45	S	0.27	12.0	12.0	-1.000	0.800	0.200	P3	-
2026	53546	2000BY6	40	278	C	0.09	15.0	5.6	0.100	180.000	90.000	P1	-
2027	-1	-	-1	-1	-	-1.00	-1.0	-1.0	-1.000	-1.000	-1.000	P3	2438 Lorre moved to high i with FIN 5008
2028	-1	-	-1	-1	-	-1.00	-1.0	-1.0	-1.000	-1.000	-1.000	P1	2782 Leonidas removed (is 144 Vibilia)
2029	144	Vibilia	38	168	C	0.07	119.0	119.0	0.500	800.000	400.000	P1	-
2030	322	Phaeo	35	677	X	0.08	66.0	65.0	0.200	370.000	200.000	P1	-
2031	-1	-	-1	-1	-	-1.00	-1.0	-1.0	-1.000	-1.000	-1.000	P1	2262 Mitidika removed
2032	6468	Welzenbach	35	2287	L	0.20	21.0	6.7	1.000	1700.000	900.000	P1	2085 Henan in P1, renamed
2033	1668	Hanna	35	1019	CX	0.05	33.0	27.0	0.200	380.000	190.000	P1	-
2034	3811	Karma	45	606	CX	0.07	34.0	30.0	0.200	320.000	160.000	P1	500 removed based on V shape
2035	2732	Witt	23	4322	S	0.20	25.0	11.0	0.700	1300.000	700.000	P1	743 removed based on V shape
2036	-1	-	-1	-1	-	-1.00	-1.0	-1.0	-1.000	-1.000	-1.000	P1	2344 Xizang removed
2037	729	Watsonia	80	226	L	0.13	55.0	51.0	0.600	1100.000	550.000	P1	-
2038	3152	Jones	30	341	T	0.05	33.0	32.0	0.020	2.500	0.500	P3	-
2039	369	Aeria	40	117	X	0.14	71.0	71.0	0.200	340.000	160.000	P1	-
2040	89	Julia	40	1756	S	0.23	148.0	148.0	0.080	130.000	65.000	P1	-
2041	1484	Postrema	70	279	CX	0.06	-1.0	-1.0	-1.000	-1.000	-1.000	P1	many large bodies: 387,599,547
2042	28	Bellona	30	958	x	0.10	148.0	147.0	0.200	370.000	185.000	P2	two large interlopers
2043	45	Eugenia	35	246	c	0.06	206.0	206.0	0.200	360.000	180.000	P2	onesided
2044	177	Irma	60	411	c	0.08	73.0	72.0	0.300	370.000	185.000	P2	large 140,180 presumed interlopers and removed
2045	194	Prokne	50	176	x	0.10	169.0	169.0	0.200	330.000	160.000	P2	194 membership unclear
2046	237	Coclestina	40	104	x	0.16	48.0	48.0	0.050	90.000	45.000	P2	albedo assumed
2047	240	Vanadis	60	17	x	0.16	91.0	91.0	0.050	90.000	45.000	P2	albedo assumed
2048	342	Endymion	20	33	c	0.04	64.0	64.0	0.010	16.000	8.000	P2	not convergent
2049	351	Yrsa	20	242	x	0.12	52.0	52.0	0.100	180.000	90.000	P2	-
2050	389	Industria	50	464	s	0.18	78.0	78.0	0.600	1000.000	500.000	P2	-
2051	446	Aeternitas	40	447	s	0.19	51.0	51.0	0.100	200.000	100.000	P2	interloper 3819 removed
2052	539	Pamina	37	81	c	0.07	45.0	44.0	0.100	200.000	100.000	P2	-

Table 1 continued on next page

Table 1 (continued)

(1)	(2)	(3)	(4)	(5)	(6)	(7)	(8)	(9)	(10)	(11)	(12)	(13)	(14)
2053	593	Titania	40	297	c	0.05	87.0	87.0	0.100	170.000	85.000	P2	onesided
2054	660	Crescentia	20	805	s	0.21	44.0	44.0	0.080	120.000	60.000	P2	alternative to Maria family, 170,695,875 removed
2055	727	Nipponia	20	510	s	0.17	38.0	37.0	0.070	110.000	60.000	P2	-
2056	801	Helwerthia	40	175	x	0.09	24.0	22.0	0.200	330.000	170.000	P2	-
2057	1048	Feodosia	40	125	c	0.06	61.0	61.0	0.080	140.000	70.000	P2	-
2058	1127	Mimi	60	82	c	0.06	48.0	48.0	0.150	240.000	120.000	P2	-
2059	1160	Illyria	30	692	s	0.26	23.0	15.0	0.800	1300.000	650.000	P2	-
2060	1347	Patria	50	132	c	0.06	31.0	30.0	0.300	500.000	250.000	P2	-
2061	2079	Jacchia	35	125	s	0.23	13.0	10.0	0.300	500.000	250.000	P2	-
2062	2927	Alamosa	20	14	s	0.16	12.0	12.0	0.002	2.200	1.000	P2	convergent
2063	3324	Avsyuk	30	222	x	0.14	22.0	21.0	0.150	260.000	130.000	P2	V shape not clear
2064	3497	Innanen	50	261	x	0.08	20.0	19.0	0.150	260.000	130.000	P2	-
2065	3567	Alvena	55	260	c	0.06	24.0	15.0	0.300	560.000	280.000	P2	-
2066	5798	Burnett	58	81	x	0.09	11.0	8.9	0.200	320.000	160.000	P2	-
2067	7233	Majella	10	17	x	0.16	10.0	10.0	0.003	1.700	1.000	P2	nice convergence
2068	7403	Choustnik	30	57	x	0.08	10.0	8.0	0.080	140.000	70.000	P2	onesided
2069	8223	Bradshaw	20	48	x	0.08	9.9	9.9	0.005	4.000	1.000	P2	convergent
2070	9332	1990SB1	10	8	s	0.32	6.2	6.2	-1.000	0.017	0.001	P3	9332 is a binary
2071	10164	Akusekijima	10	18	s	0.28	8.3	8.3	-1.000	3.000	0.500	P3	-
2072	11014	Svatopluk	50	157	x	0.09	15.0	14.0	0.120	200.000	100.000	P2	large 13056,27312 removed
2073	12586	Shukla	20	25	s	0.19	5.7	5.6	0.004	1.500	1.000	P2	convergent
2074	15104	2000BV3	30	78	c	0.08	17.0	16.0	0.030	60.000	30.000	P2	-
2075	16472	1990OE5	7	58	c	0.05	14.0	11.0	0.020	40.000	20.000	P2	-
2076	16940	1998GC3	20	40	s	0.19	-1.0	-1.0	-1.000	-1.000	-1.000	P2	large 6094, interpretation unclear
2077	21591	1998TA6	15	47	s	0.26	6.7	5.3	0.013	20.000	10.000	P2	-
2078	22766	1999AE7	10	5	x	0.16	5.1	5.1	-1.000	0.750	0.750	P3	-
2079	26170	Kazuhiko	10	9	s	0.35	5.0	4.9	0.006	1.000	1.000	P3	not clear
2080	30718	Records	40	94	c	0.06	10.0	9.2	0.050	90.000	45.000	P2	54991 removed
2081	32983	1996WU2	20	50	s	0.25	6.8	5.8	0.050	80.000	40.000	P2	-
2082	42357	2002CS52	40	216	s	0.20	-1.0	-1.0	0.050	80.000	40.000	P2	several large bodies, 678,9017,28356
2083	49362	1998WW16	30	68	s	0.27	4.4	3.1	0.020	34.000	17.000	P2	large 51341
2084	53209	1999CQ75	20	188	c	0.05	13.0	9.7	0.040	70.000	35.000	P2	large 32137 removed
2085	54934	2001OH105	50	37	c	0.08	5.9	5.6	0.050	80.000	40.000	P2	-
2086	190237	2007DM10	50	41	x	0.16	1.9	1.8	-1.000	-1.000	-1.000	P2	large 190237 offset, no V shape
2087	249576	1995FH2	30	78	c	0.04	6.2	3.5	0.050	90.000	45.000	P2	-

Table 1 continued on next page

Table 1 (continued)

(1)	(2)	(3)	(4)	(5)	(6)	(7)	(8)	(9)	(10)	(11)	(12)	(13)	(14)
2088	325224	2008GK38	20	90	x	0.16	2.5	2.0	0.010	4.500	1.500	P2	convergent, 435544 in P2
2089	-1	2006QX49	20	11	x	0.16	1.7	1.7	-1.000	-1.000	-1.000	P2	young, clustered angles, 2006QX49 interloper?
2090	5478	Wartburg	10	5	x	0.16	8.8	8.8	-1.000	0.400	0.200	P3	-
2091	18777	Hobson	10	66	x	0.16	4.0	3.1	-1.000	2.000	2.000	P3	-
2092	66583	Nicandra	10	13	c	0.05	6.2	6.0	-1.000	1.500	1.500	P3	-
2093	2258	Viipuri	10	8	c	0.04	26.0	26.0	-1.000	2.500	3.500	P3	-
2094	1346	Gotha	10	7	s	0.28	14.0	14.0	-1.000	0.600	0.100	P3	-
2095	5971	Tickell	10	13	s	0.37	8.7	8.7	-1.000	1.500	0.300	P3	in Eunomia
2096	16126	1999XQ86	10	6	s	0.34	6.6	6.6	-1.000	0.150	0.050	P3	-
2097	22216	1242T-2	10	5	x	0.11	5.9	5.9	-1.000	0.500	0.200	P3	in Juno
2098	45765	2000LJ3	10	3	x	0.46	4.1	4.1	-1.000	0.600	0.100	P3	albedo may be wrong
2099	46162	2001FM78	10	4	x	0.16	3.0	2.9	-1.000	0.500	0.300	P3	in Maria, not clear
2100	81291	2000FA70	10	6	x	0.16	2.8	2.8	-1.000	0.300	0.300	P3	complicated convergence
2101	103022	1999XU109	10	7	x	0.16	2.9	2.9	-1.000	3.000	1.000	P3	two nodal groups
2102	114555	2003BN44	7	58	c	0.05	-1.0	-1.0	-1.000	3.000	1.000	P3	in Dora, several large bodies
2103	128637	2004RK22	10	4	x	0.16	2.2	2.1	-1.000	0.250	0.250	P3	-
2104	209165	2003UC86	10	4	x	0.16	1.4	1.3	-1.000	1.000	1.000	P3	-
2105	267333	2001UZ193	10	3	x	0.16	1.3	1.2	-1.000	1.500	1.500	P3	convergence unclear
2106	346662	2008YG14	10	4	x	0.16	1.5	1.5	-1.000	0.800	0.500	P3	-
2107	384028	2008UE119	10	3	x	0.16	1.5	1.5	-1.000	0.500	0.500	P3	double convergence
<i>Outer Main Belt, <math>a &gt; 2.82</math> AU, <math>i &lt; 17.5^\circ</math></i>													
3001	10	Hygiea	50	12750	CB	0.07	447.0	433.0	1.000	2400.000	1200.000	P1	several large interlopers?
3002	24	Themis	50	13627	C	0.07	280.0	202.0	1.500	3500.000	1000.000	P1	-
3003	87	Sylvia	100	1649	X	0.05	309.0	272.0	1.000	2900.000	1500.000	P1	beyond 2:1, large 107
3004	511	Davidia	55	444	C	0.07	298.0	298.0	0.200	500.000	250.000	P1	replaced 137 Meliboea, Masiero et al. (2013)
3005	158	Koronis	30	12208	S	0.23	102.0	48.0	1.500	3000.000	1500.000	P1	PZ (pristine zone)
3006	221	Eos	28	33006	K	0.13	208.0	96.0	1.000	2000.000	1000.000	P1	large halo, younger family near 3.17 au
3007	283	Emma	30	1226	C	0.05	137.0	134.0	0.200	450.000	180.000	P1	skips over a secular resonance
3008	293	Brasilia	50	3466	X	0.16	-1.0	-1.0	0.100	200.000	100.000	P1	PZ, asymmetric V shape, 293 may be interloper
3009	490	Veritas	20	6375	CPD	0.07	120.0	91.0	0.070	8.300	0.100	P3	gamma dust band source
3010	832	Karin	10	3863	S	0.20	33.0	17.0	0.030	5.720	0.050	P3	PZ, beta dust band, includes Koronis2
3011	845	Naema	35	1313	C	0.06	63.0	57.0	0.200	410.000	200.000	P1	PZ
3012	1400	Tirela	40	14114	S	0.07	-1.0	-1.0	0.750	1700.000	850.000	P1	many large bodies
3013	3556	Lixiaohua	35	6456	CX	0.05	-1.0	-1.0	0.200	480.000	240.000	P1	many large bodies
3014	9506	Telramund	28	350	S	0.21	19.0	6.6	0.100	220.000	110.000	P1	smaller population than in P1

Table 1 continued on next page

Table 1 (continued)

(1)	(2)	(3)	(4)	(5)	(6)	(7)	(8)	(9)	(10)	(11)	(12)	(13)	(14)
3015	18405	1993FY12	40	524	CX	0.17	-1.0	-1.0	0.100	160.000	80.000	P1	large 29903
3016	627	Charis	60	3444	C	0.08	63.0	45.0	0.300	600.000	300.000	P1	PZ
3017	778	Theobalda	30	4848	CX	0.06	63.0	54.0	0.100	6.900	2.300	P3	-
3018	1189	Terentia	40	541	C	0.06	62.0	61.0	0.200	300.000	150.000	P1	PZ
3019	10811	Lau	50	830	S	0.13	11.0	7.7	0.070	140.000	70.000	P1	PZ, cut by a secular resonance
3020	656	Beagle	20	638	C	0.07	-1.0	-1.0	0.050	70.000	35.000	P3	alpha dust band?, 656 and other larg interlopers
3021	158	Koronis2	10	3863	S	0.20	-1.0	-1.0	-1.000	10.000	5.000	P3	PZ, includes Karin, Vokrouhlický et al. (2026)
3022	81	Terpsichore	70	249	C	0.05	122.0	122.0	0.400	780.000	390.000	P1	PZ, V shape not clear
3023	709	Fringilla	100	498	X	0.06	-1.0	91.0	0.300	600.000	300.000	P1	PZ, large 776 and 1191
3024	5567	Durisen	80	156	X	0.04	42.0	40.0	0.200	420.000	210.000	P1	PZ
3025	5614	Yakovlev	100	330	C	0.05	-1.0	13.0	0.200	400.000	200.000	P1	PZ, V shape not clear
3026	7481	SanMarcello	60	248	X	0.19	-1.0	-1.0	0.400	410.000	200.000	P1	PZ, super large 22 Kalliope
3027	15454	1998YB3	60	373	CX	0.05	-1.0	16.0	0.070	140.000	70.000	P1	PZ, several large bodies
3028	15477	1999CG1	70	633	S	0.10	-1.0	-1.0	-1.000	-1.000	-1.000	P1	PZ, interpretation unclear, old and depleted?
3029	36256	1999XT17	50	661	S	0.20	21.0	10.0	1.000	2100.000	1000.000	P1	PZ, several large bodies
3030	96	Aegle	40	203	CX	0.07	144.0	143.0	0.400	900.000	450.000	P1	-
3031	375	Ursula	45	5228	CX	0.07	-1.0	-1.0	-1.000	-1.000	-1.000	P1	contains 618 Elfriede family, interpretation unclear
3032	618	Elfriede	30	1081	C	0.06	132.0	131.0	0.050	120.000	60.000	P1	inside of 375 Ursula
3033	918	Itha	80	155	S	0.19	-1.0	-1.0	0.300	600.000	300.000	P1	PZ
3034	3438	Inarradas	50	78	CX	0.08	35.0	25.0	0.300	670.000	340.000	P1	depleted
3035	7468	Anfimov	40	103	S	0.14	15.0	10.0	0.300	670.000	340.000	P1	depleted
3036	1332	Marconia	30	275	CX	0.05	52.0	52.0	0.030	70.000	35.000	P1	-
3037	86	Semele	40	642	CX	0.05	120.0	120.0	0.050	120.000	60.000	P1	previously known as 106302 2000UJ87
3038	589	Croatia	30	166	X	0.06	97.0	96.0	0.500	1200.000	600.000	P1	-
3039	926	Imhilde	50	451	CX	0.05	47.0	46.0	0.150	320.000	160.000	P1	-
3040	20672	Gibbs	10	35	-	-1.00	-1.0	-1.0	-1.000	1.500	1.000	P1	P/2012 Gibbs, Novaković et al. (2014)
3041	816	Juliana	50	314	CX	0.08	52.0	50.0	0.400	860.000	430.000	P1	-
3042	174	Phaedra	60	170	x	0.12	75.0	74.0	0.200	400.000	200.000	P2	PZ
3043	321	Florentina	10	209	S	0.19	34.0	34.0	0.200	400.000	200.000	P2	PZ, also known as Koronis4
3044	392	Wilhelmina	40	45	c	0.05	69.0	69.0	0.050	100.000	50.000	P2	PZ
3045	924	Toni	50	50	x	0.10	50.0	50.0	0.050	100.000	50.000	P2	PZ
3046	1289	Kutaissi	10	371	s	0.25	-1.0	-1.0	0.100	150.000	75.000	P3	PZ, also known as Koronis3
3047	3787	Aivazovskij	15	12	s	0.33	12.0	12.0	0.010	40.000	20.000	P2	PZ
3048	4471	Graculus	50	136	x	0.13	12.0	11.0	0.070	140.000	70.000	P2	PZ
3049	11048	1990QZ5	50	35	s	0.17	9.1	8.4	0.050	100.000	50.000	P2	PZ

Table 1 continued on next page

Table 1 (continued)

(1)	(2)	(3)	(4)	(5)	(6)	(7)	(8)	(9)	(10)	(11)	(12)	(13)	(14)
3050	19093	1979MM3	90	71	c	0.06	-1.0	-1.0	0.500	2000.000	1000.000	P2	PZ, depleted
3051	26369	1999CG62	50	43	c	0.05	24.0	24.0	0.015	30.000	15.000	P2	PZ
3052	31810	1999NR38	60	103	x	0.13	11.0	8.0	0.200	400.000	200.000	P2	PZ, depleted
3053	77873	2001SQ46	50	21	x	0.08	6.8	6.6	0.020	40.000	20.000	P2	PZ
3054	78225	2002OS10	60	88	s	0.16	6.4	4.7	0.250	500.000	250.000	P2	PZ
3055	11945	Aletta	70	294	x	0.07	47.0	46.0	0.300	600.000	300.000	P2	PZ, 242 removed, renamed 211774
3056	217472	2005WV105	40	37	x	0.10	3.6	2.7	0.050	100.000	50.000	P2	PZ
3057	52	Europa	50	250	C	0.06	320.0	320.0	-1.000	-1.000	-1.000	P2	cratering on Europa?
3058	106	Dione	55	261	c	0.06	140.0	140.0	0.500	1200.000	600.000	P2	-
3059	260	Huberta	70	190	c	0.04	89.0	86.0	0.250	700.000	350.000	P2	-
3060	286	Iclea	50	143	c	0.06	83.0	83.0	0.040	100.000	50.000	P2	-
3061	414	Liriope	70	14	c	0.03	89.0	89.0	0.030	90.000	45.000	P2	-
3062	522	Helga	200	34	c	0.04	84.0	84.0	0.300	700.000	350.000	P1	beyond 2:1
3063	633	Zelima	10	88	s	0.17	43.0	43.0	-1.000	3.000	1.000	P3	-
3064	690	Wratislavia	30	820	c	0.05	131.0	131.0	0.050	240.000	120.000	P2	-
3065	850	Altona	60	73	c	0.07	60.0	60.0	0.200	430.000	220.000	P2	-
3066	885	Ulrike	30	45	x	0.10	29.0	29.0	0.070	160.000	80.000	P2	onesided
3067	991	McDonalda	20	260	c	0.06	-1.0	40.0	0.100	240.000	120.000	P2	many large bodies
3068	1357	Khama	30	62	c	0.05	40.0	40.0	0.060	150.000	75.000	P2	-
3069	1461	Jean-Jaques	30	174	x	0.09	42.0	42.0	0.040	140.000	70.000	P2	-
3070	1524	Joensuu	40	201	x	0.09	51.0	49.0	0.150	350.000	180.000	P2	onesided, two large bodies
3071	1599	Giornus	25	322	c	0.06	50.0	47.0	0.150	350.000	350.000	P2	onesided
3072	2458	Veniakaverin	30	177	c	0.05	26.0	22.0	0.070	170.000	80.000	P2	-
3073	2562	Chaliapin	22	271	s	0.16	-1.0	18.0	0.200	430.000	220.000	P2	many large bodies
3074	3310	Patsy	15	826	s	0.16	-1.0	21.0	0.120	220.000	110.000	P2	onesided, many large bodies
3075	3803	Tuchkova	10	7	c	0.04	42.0	42.0	-1.000	-1.000	-1.000	P2	not convergent
3076	4291	Kodaihasu	20	16	x	0.10	18.0	18.0	0.005	5.000	1.500	P2	convergent
3077	15537	2000AM199	20	252	x	0.14	13.0	10.0	0.030	70.000	30.000	P2	4897 and 36101 offset and removed
3078	5228	Maca	30	47	c	0.07	15.0	14.0	0.100	230.000	120.000	P2	onesided
3079	6924	Fukuui	80	146	c	0.05	33.0	30.0	0.200	550.000	180.000	P2	-
3080	7504	Kawakita	10	19	c	0.07	10.0	10.0	0.006	15.000	8.000	P2	not convergent
3081	8737	Takehiro	40	569	c	0.07	-1.0	19.0	0.200	470.000	240.000	P2	many large bodies outside V
3082	9522	Schlichting	100	9	c	0.07	-1.0	-1.0	-1.000	-1.000	-1.000	P2	interpretation unclear
3083	12911	Goodhue	18	132	c	0.07	16.0	15.0	0.025	60.000	30.000	P2	-
3084	20674	1999VT1	10	35	x	0.10	12.0	11.0	0.005	2.000	0.500	P3	20674 offset

Table 1 continued on next page

Table 1 (continued)

(1)	(2)	(3)	(4)	(5)	(6)	(7)	(8)	(9)	(10)	(11)	(12)	(13)	(14)
3085	29880	Andytran	20	44	x	0.09	9.4	7.3	0.020	50.000	25.000	P2	-
3086	34216	2000QK75	20	22	c	0.04	12.0	12.0	0.006	1.500	0.700	P3	onesided
3087	37455	4727P-L	40	285	x	0.08	-1.0	-1.0	0.080	200.000	100.000	P2	large 28876
3088	48412	1986QN1	60	100	x	0.12	-1.0	-1.0	0.200	430.000	220.000	P2	very large 478
3089	48506	1993FO10	20	90	x	0.08	11.0	7.1	0.020	50.000	25.000	P2	large 91155
3090	63235	2001BV20	60	35	x	0.08	-1.0	-1.0	0.120	360.000	180.000	P2	large 46305
3091	77882	2001SV124	45	316	x	0.09	-1.0	-1.0	-1.000	-1.000	-1.000	P2	interpretation unclear
3092	157940	1999XU240	10	19	c	0.04	7.3	4.7	0.020	40.000	20.000	P2	-
3093	352479	2008BO31	30	50	c	0.06	-1.0	-1.0	-1.000	-1.000	-1.000	P2	interpretation unclear
3094	365736	2010WK8	50	40	x	0.10	6.7	4.4	0.100	270.000	140.000	P2	-
3095	15156	2000FK38	50	11	c	0.07	12.0	10.0	-1.000	-1.000	-1.000	P3	needs confirmation
3096	22280	Mandragora	15	67	c	0.05	11.0	10.0	-1.000	1.500	1.500	P3	complicated convergence
3097	5950	Leukippos	10	16	s	0.19	10.0	10.0	-1.000	1.300	0.500	P3	in Koronis
3098	26046	2104T-2	10	3	s	0.23	3.1	3.1	-1.000	0.700	0.200	P3	in Koronis
3099	28965	2001FF162	10	6	s	0.23	3.3	3.3	-1.000	1.750	0.750	P3	in Koronis
3100	238659	2005EG114	10	3	x	0.10	2.6	2.6	-1.000	0.500	0.200	P3	-
3101	349030	2006VA32	10	3	x	0.10	2.6	2.3	-1.000	0.400	0.200	P3	-
3102	503256	2015KL76	10	14	x	0.10	3.0	2.1	-1.000	1.500	1.500	P3	-
3103	63530	2001PG20	90	419	c	0.05	-1.0	-1.0	0.300	600.000	300.000	P1	PZ
<i>Inner Main Belt, <math>a &lt; 2.5 AU, i &gt; 17.5^\circ</math></i>													
4001	25	Phocaea	150	8406	S	0.22	-1.0	-1.0	-1.000	-1.000	-1.000	P1	practically the whole Phocaea group
4002	434	Hungaria	35	3914	E	0.35	17.0	13.0	0.200	180.000	90.000	P1	moved from FIN 0003
4003	3001	Michelangelo	200	42	s	0.21	9.9	9.8	0.150	200.000	100.000	P2	-
4004	316974	2001FP147	150	53	c	0.03	5.9	4.0	0.050	70.000	35.000	P2	-
4005	3854	George	130	261	E	0.35	7.7	3.2	0.100	90.000	45.000	P2	in Hungarias
4006	4765	Wasserburg	10	8	E	0.35	1.9	1.8	-1.000	0.350	0.250	P3	in Hungarias
4007	6084	Bascom	10	10	s	0.22	6.5	6.5	-1.000	0.500	0.300	P3	Bascom is a binary
4008	63440	2001MD30	20	7	E	0.35	2.0	1.9	-1.000	0.500	0.500	P3	in Hungarias
4009	70208	1999RX33	20	16	s	0.21	2.4	1.7	-1.000	0.850	0.150	P3	-
4010	41331	1999XB232	20	23	s	0.21	5.6	5.6	-1.000	1.700	0.500	P3	in Phocaea
4011	51866	2001PH3	10	6	s	0.25	4.1	4.0	-1.000	0.500	0.300	P3	-
4012	86419	2000AL245	10	5	E	0.35	1.6	1.6	-1.000	0.650	0.650	P3	in Hungarias
4013	100416	Syang	10	3	E	0.35	1.4	1.4	-1.000	0.150	0.150	P3	in the Hungaria family
4014	180023	2003AU16	10	3	E	0.35	1.0	1.0	-1.000	0.040	0.020	P3	in Hungarias
4015	267721	2003CL11	10	3	E	0.35	0.8	0.8	-1.000	0.002	0.002	P3	in Hungarias

Table 1 continued on next page

Table 1 (continued)

(1)	(2)	(3)	(4)	(5)	(6)	(7)	(8)	(9)	(10)	(11)	(12)	(13)	(14)	
4016	368103	2013EN	10	3	E	0.35	0.6	0.6	-1.000	0.500	0.500	P3	in the Hungaria family	
4017	481085	2005SX233	10	6	s	0.21	1.1	1.1	-1.000	0.500	0.500	P3	-	
4018	1963	Bezovec	65	354	s	0.28	45.0	45.0	0.300	400.000	200.000	P2	in Phocaea	
4019	6065	Chesneau	60	351	s	0.29	17.0	5.5	0.600	800.000	400.000	P2	in Phocaea	
							<i>Middle Main Belt, 2.5 &lt; a &lt; 2.82 AU, i &gt; 17.5°</i>							
5001	2	Pallas	300	515	B	0.14	512.0	512.0	1.000	1800.000	900.000	P1	-	
5002	148	Gallia	150	1346	S	0.17	100.0	-1.0	0.500	900.000	450.000	P1	large 71 and 247	
5003	480	Hansa	100	5214	S	0.27	59.0	56.0	0.300	500.000	250.000	P1	925 assumed interloper and removed	
5004	686	Gersuind	53	567	S	0.13	47.0	42.0	0.300	480.000	240.000	P1	-	
5005	945	Barcelona	100	5428	S	0.26	31.0	26.0	0.200	330.000	170.000	P1	well defined left ear	
5006	1222	Tina	100	1035	X	0.13	30.0	29.0	0.100	170.000	50.000	P1	-	
5007	4203	Brucato	110	202	CX	0.07	27.0	18.0	0.400	500.000	250.000	P1	depleted	
5008	5438	Lorre	20	150	C	0.05	24.0	24.0	0.010	4.000	2.000	P3	moved here to high i	
5009	183	Istria	80	301	s	0.25	31.0	31.0	0.150	280.000	140.000	P2	-	
5010	78705	2002TE180	10	24	x	0.16	4.6	4.6	0.020	35.000	18.000	P2	-	
5011	101567	1999AW22	50	293	s	0.20	-1.0	-1.0	-1.000	-1.000	-1.000	P2	101567 discordant with possible V shape	
5012	236657	2006KU114	70	302	c	0.06	-1.0	-1.0	0.100	180.000	90.000	P2	large 101679	
							<i>Outer Main Belt, a &gt; 2.82 AU, i &gt; 17.5°</i>							
6001	31	Euphrosyne	100	15488	C	0.06	304.0	280.0	0.700	1700.000	900.000	P1	-	
6002	702	Alauda	80	3556	B	0.07	-1.0	201.0	1.500	3500.000	1700.000	P1	-	
6003	909	Ulla	120	103	X	0.05	103.0	103.0	0.350	2100.000	1000.000	P1	depleted	
6004	1303	Luthera	40	1116	X	0.04	97.0	92.0	0.200	500.000	350.000	P1	-	
6005	780	Armenia	40	393	C	0.05	102.0	102.0	0.150	350.000	180.000	P1	-	
6006	350	Ornamenta	70	716	c	0.07	101.0	100.0	0.500	1200.000	600.000	P1	-	
6007	386	Siegena	100	168	c	0.06	147.0	147.0	0.150	300.000	150.000	P1	PZ	
6008	704	Interammia	50	413	F	0.06	332.0	332.0	0.150	340.000	170.000	P1	V shape unclear	
6009	754	Malabar	60	79	Ch	0.05	44.0	44.0	0.050	100.000	50.000	P1	-	
6010	1312	Vassar	30	21	x	0.10	31.0	31.0	0.050	100.000	50.000	P1	onesided	
6011	1390	Abastumani	40	65	c	0.06	108.0	108.0	0.050	140.000	70.000	P1	beyond 2:1	
6012	7605	Cindygraber	30	85	c	0.06	47.0	45.0	0.025	60.000	30.000	P1	-	
6013	77899	2001TS117	200	257	s	0.16	16.0	7.1	0.200	500.000	250.000	P1	-	
6014	126948	2002FX3	30	14	c	0.06	8.2	6.6	0.020	36.000	18.000	P1	V shape not clear	
6015	37981	1998HD130	90	419	c	0.05	-1.0	-1.0	-1.000	-1.000	-1.000	P2	PZ, 37981 offset, hint of V	
6016	1323	Tugela	50	412	c	0.04	91.0	91.0	0.080	200.000	100.000	P2	-	



**Table 2.** Example of a family membership file. The table lists first 15 lines from the file `inner_4_Vesta.fam3`. The full file is available at <https://www.boulder.swri.edu/~davidn/Proper25>. It lists 27121 members of the Vesta family (FIN 1001) identified with the HCM cutoff  $d_{\text{cut}} = 35 \text{ m s}^{-1}$ . See Section 2.7 for a definition of different columns.

(1)	(2)	(3)	(4)	(5)	(6)	(7)	(8)	(9)
2.361512	0.099452	0.111023	36.882605	-39.610314	3.220	110	00004	4
2.361012	0.099048	0.110782	36.884715	-39.590248	15.630	17	46696	46696
2.362293	0.100277	0.110644	36.929856	-39.689733	15.430	20	58454	58454
2.362667	0.099859	0.111384	36.926802	-39.662969	16.270	16	94952	94952
2.364954	0.099838	0.110849	37.017279	-39.768000	17.320	12	b0912	370912
2.359748	0.100057	0.110159	36.871141	-39.579834	17.420	10	j0004	450004
2.363977	0.098659	0.111137	36.971241	-39.696500	18.320	8	r5947	535947
2.360996	0.099878	0.110858	36.882022	-39.602690	17.820	10	~01do	626312
2.363085	0.098985	0.111650	36.927794	-39.667195	18.590	7	K17X72Y	2017XY72
2.362002	0.099983	0.110356	36.939246	-39.652123	18.830	3	K19P87G	2019PG87
2.357527	0.098684	0.110713	36.766754	-39.444188	17.840	12	K02PF0H	2002PH150
2.362296	0.101011	0.111688	36.892056	-39.711294	18.560	7	K15P98A	2015PA98
2.362435	0.101125	0.110924	36.925802	-39.727003	18.710	6	K21GB8D	2021GD118
2.361728	0.099745	0.112360	36.859142	-39.631252	18.570	6	K13CN8F	2013CF238
2.359805	0.099840	0.112109	36.802075	-39.561819	18.320	7	K14G83M	2014GM83

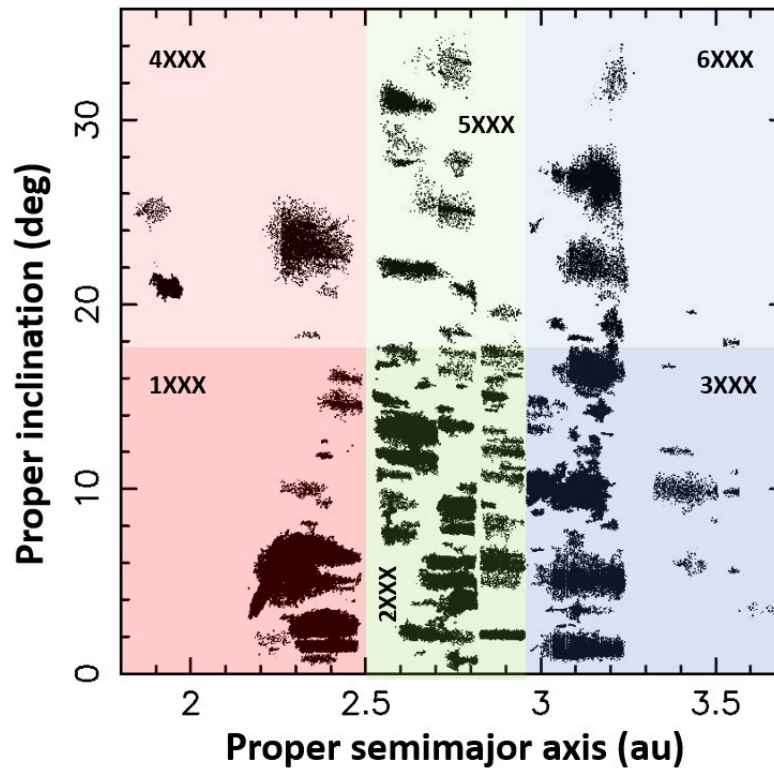


**Figure 1.** The 335 collisional families reported in this catalog. The main belt is divided into the inner belt ( $a_p < 2.5$  au; red), middle belt ( $2.5 < a_p < 2.82$  au; green) and outer belt ( $a_p > 2.82$  au; blue). The upper part of the belt with  $i_p > 17.5$  deg is highlighted by lighter colors. The black dots show members of the identified families. The labels indicate the proposed FIN designations of families in different main belt regions.

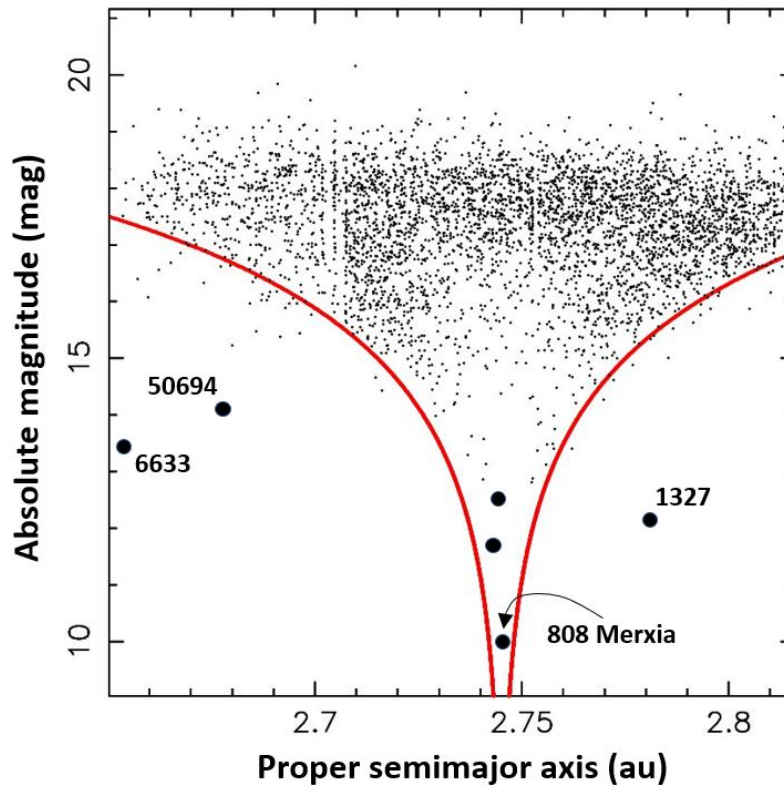


**Figure 2.** The best-fit V envelope for the Merxia family ( $C_0 = 3 \times 10^{-5}$  AU, red lines; the black dots are the HCM family members). Asteroid 808 Merxia is perfectly centered in the V shape envelope and is likely the true largest member in the family. Asteroids 1327, 6633 and 50694 are suspected interlopers. The Merxia family age is estimated to be  $\sim 500$  Myr from Eq. (3), but the previous detailed Yarkovsky-YORP chronology modeling established  $t_{\text{age}} = 250 \pm 100$  Myr (Vokrouhlický et al. 2006). This illustrates a case where the V envelope method can significantly overestimate the true age of a family (due to the neglected effect of ejection velocities).

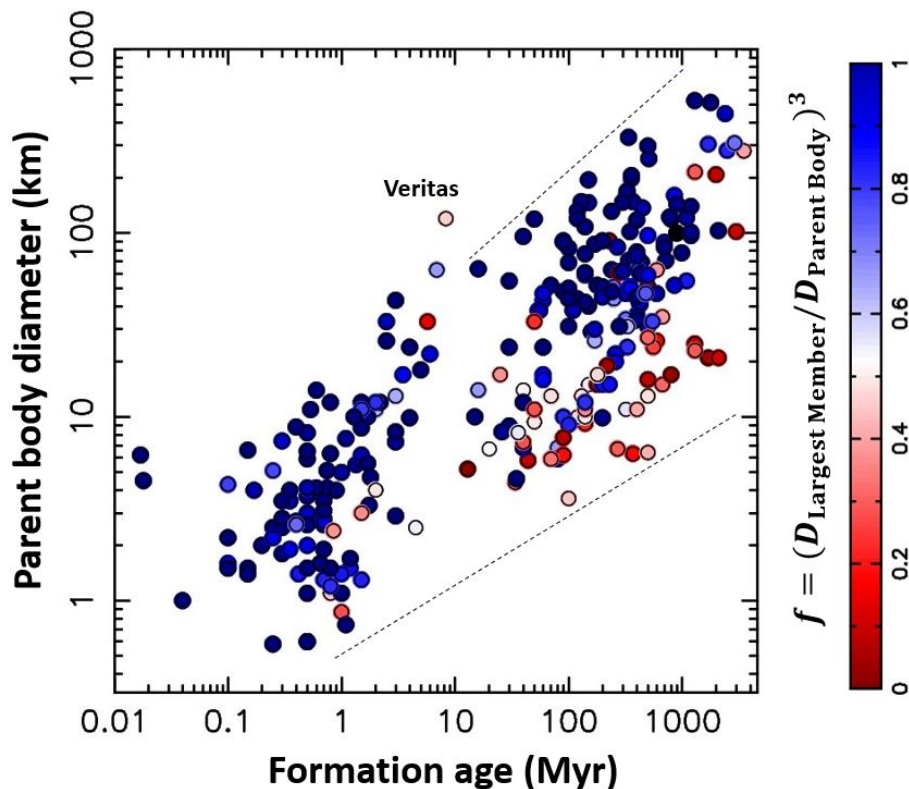


**Figure 3.** The estimated parent body diameters and formation ages of families reported in this catalog. See Sections 2.5 and 2.6 for the method used to determine these parameters. The color indicates  $f = (D_{\text{LM}}/D_{\text{PB}})^3$  where  $D_{\text{LM}}$  and  $D_{\text{PB}}$  are the estimated largest-member and parent-body diameters, respectively. The families produced by the cratering collisions appear as dark blue dots; the catastrophic breakups with  $f < 0.5$  are shown in red.